Journal of the Indian Society of Remote Sensing (May 2024) 52(5):1003–1018
https://doi.org/10.1007/s12524-024-01853-x

RESEARCH ARTICLE

Drought Characterization Using the Grace Terrestrial Water Storage Deficit in Turkey

Emre Topçu[1]

Received: 14 February 2022 / Accepted: 13 March 2024 / Published online: 8 April 2024
© Indian Society of Remote Sensing 2024

Abstract

Drought is a climatic event that has negative environmental effects. Detecting the drought in a region enables more effective water resources management in that region. This study was designed to carry out drought analysis for 98 months in the period of February 2010 and November 2020 in designated areas within the region determined in Turkey which is located in the temperate zone of the northern hemisphere. The analyzed data included terrestrial water storage anomaly (TWSA) values derived from Gravity Recovery and Climate Experiment (GRACE) and GRACE-FO (Follow On) satellites and monthly total precipitation values obtained from the PERSIANN system (Precipitation Estimation from Remotely Sensed Information using Artificial Neural Networks). Drought analysis was identified by utilizing the water storage deficit index (WSDI) and standardized precipitation index (SPI). The drought index values were compared with 5 different (The Arctic Oscillation (AO), The North Atlantic Oscillation (NAO), The Multivariate ENSO (El-Nino/Southern Oscillation) Index (MEI), The Oceanic Nino Index (ONI) and The Southern Oscillation Index (SOI)) atmospheric/oceanic climate indexes. The results of this study indicate that the years with the highest water deficit are 2014, 2018 and 2020. From 2010 to 2020, the equivalent water thickness (EWT) has decreased from + 1.5 to − 11.1 cm. Whereas wetness was observed throughout Turkey between the years 2010–2013, it was revealed that droughts occurred between the years 2014–2020. The findings of this study also showed that there was a significant correlation (at a significance level) among WSDI and AO, NAO and ONI indexes.

Keywords Climatic index · Drought index · GRACE · SPI · Turkey · Water storage deficit

Introduction

Drought is a versatile climatic event that occurs naturally at a wide variety of spatio-temporal scales. Drought, which has negative environmental, social and economic effects, generally causes a decrease in agricultural production, production and job losses, more common dust storms, more intense forest fires and many other adverse events (Hosseini-Moghari et al., 2020). Due to the complexity of drought and its factors, numerous techniques are used to identify and monitor drought. Drought indexes are suitable tools used in assessing drought, in investigating the social and ecological effects of drought, as well as deciding on drought prevention and reduction stages. Many drought indexes used to detect drought in the world have to rely on the accuracy of meteorological input parameters. However, if ground observations, such as precipitation and ground characteristics, are sparse in a region, the drought indexes used become unreliable. For this reason, drought indices using drought-related parameters (such as ground humidity, terrestrial water storage, equivalent water thickness) derived by remote sensing via satellite are recommended as complementary to frequently used drought indexes (Zhao et al., 2017).

Drought is characterized by a total lack of water (such as ground water, surface water and groundwater). Traditionally, regional drought assessment is carried out with parameters derived from meteorology stations installed on earth. However, long-term observation in large areas is both limited and costly. In recent years, remote sensing approaches have been developed to accurately understand the formation and regional change of drought-related parameters (Yu et al., 2019). Remote sensing drought indices have opened a new path in drought monitoring and detection at both global and regional scale.

✉ Emre Topçu
emretopcu01@gmail.com

[1] Civil Engineering Department, Kafkas University, 36100 Kars, Turkey

NASA's (National Aeronautics and Space Administration) The Gravity Recovery and Climate Experiment (GRACE) satellite was launched in March 2002 and it obtained the changes in the earth's gravitational field with detailed measurements and associated these measurements with terrestrial water storage (TWS) changes in the land areas. This represents a new source of information on hydrological properties (Sun et al., 2018). The GRACE satellite completed its mission in 2017, and on May 22, 2018, the GRACE-FO (Follow On) satellite was launched and took over the mission. GRACE missions are to measure the gravitational changes on the surface of the earth by creating a new gravitational field map every 30 days. Monthly changes in mass are the cause of the observed monthly changes in gravity. The mass changes can be thought of as being concentrated in a very thin layer of changes in water thickness near the Earth's surface. Actually, most of the monthly gravity changes result from water storage changes, from the movement of the oceans, atmosphere and land ice, and from mass exchanges between these parts of the Earth system. Their vertical magnitude is measured in centimetres of equivalent water thickness, much smaller than the Earth's radius or the horizontal scales of change, measured in kilometres. Equivalent water thickness (EWT) represents the total terrestrial water storage anomaly (TWSA) in ground moisture, snow, surface water (such as rivers, lakes, reservoirs) groundwater and aquifers. In TWSA values, a negative value indicates a water storage deficit. Each monthly deficit represents the amount of water required to return to normal water storage conditions (Thomas et al., 2014). Since the change in water resources directly affects the parameters of the hydrological cycle occurring in the atmosphere, the equivalent water thickness measured by GRACE provides significant information in terms of drought.

Time-varying gravitational changes are caused by postglacial recovery, change in atmospheric mass and redistribution of the distributions of water, snow and ice on land and in the ocean. Satellite is an extremely valuable tool in remote sensing and characterization of drought, as it can measure from regional to global scale. Because many drought detection techniques cannot observe the water storage variability in all hydrological components (Swenson & Wahr, 2003).

Drought can be triggered by globally accepted climatic indexes, or oscillations. Climate index defines the state of the climate and changes in the climate system. It is represented by a time series, and each point in the time series corresponds to an index value. Each climate index is based on specific parameters and only describes a particular aspect of the climate. Therefore, many climate indexes have been defined. For each climate index, there are descriptive parameters using climate elements. These are atmospheric parameters such as air pressure, air temperature, precipitation, solar radiation that affect the characteristics of the climate system and other non-atmospheric but measurable descriptive parameters such as sea surface temperature and ice cover (Gürsoy, 2018). The most widely known climate indices are the Arctic Oscillation Index (AO), Multivariate ENSO Index (MEI), North Atlantic Oscillation Index (NAO), Oceanic Nino Index (ONI) and Southern Oscillation Index (SOI).

Khorrami et al. (2023) hypothesise that for a practical hydrological investigation of water storage variability, the original GRACE/GRACE-FO observations can be used in combination with the large-scale hydrological models. In their study, using the GRACE/GRACE-FO estimates and the hydroclimatic model, the spatio-temporal variations of TWS over the different regions of Turkey were evaluated. Using the scPDSI and GRACE-derived Water Storage Deficit (WSD) indices, the relationships between drought and variations in water storage over the study area were also examined. Their study found declining trends in TWS in all geographic regions of the country, indicating continued water storage losses over the last 18 years, from 2003 through 2020. However, as previously mentioned, climatic oscillations affecting global climate conditions change the hydrometeorological structure of the earth. Therefore, the relationship between global climate oscillations and GRACE data should also be investigated. The present study is designed to fulfil this gap.

Turkey is located in the northern hemisphere at the crossroads of Europe and Asia. It has different climate types because it is surrounded by the sea on three sides and is higher than the sea level. There are drought events that differ in continuity and intensity due to different climatic conditions. There are not many studies in Turkey using GRACE satellite data. Lenk (2013), Ahi and Jin (2019) can be given as examples of the main hydrological studies conducted with the GRACE satellite in Turkey. In this study, hydrological drought characterization of Turkey was carried out by using terrestrial water storage anomaly (equivalent water thickness) values derived from GRACE and GRACE-FO satellites between February 2010 and November 2020. With the help of equivalent water thicknesses observed through the GRACE and GRACE-FO satellites, it was determined by using the locations of meteorological stations in 81 across Turkey. This study also investigated the correlation among AO, MEI, NAO, ONI and SOI and Water Storage Deficit Index (WSDI) (Thomas et al., 2014), which is thought to affect Turkey climatically. In addition, the results were compared with WSDI and the Standardized Precipitation Index (SPI) (McKee et al., 1993) i.e. a meteorological drought index.

Material and Method

Material

GRACE Data

Since the GRACE satellites were launched in 2002, they have accurately detected the gravitational changes caused by adjustments in the terrestrial water storage (TWS) column due to various hydrological processes. TWS includes water stored in all forms on the land surface and below. Since GRACE satellites lack vertical analysis to distinguish changes in various hydrosphere components separately, they can only identify changes in the column-integrated water body. Global TWS estimates derived from temporal gravitational field changes observed by GRACE satellites require post-processing techniques such as scaling, smoothing, trancation, and eliminating correlational errors (Chen et al., 2005; Landerer and Swenson (2012); Wahr et al., 2004; Tang et al., 2014; Sinha et al., 2017). Infiltration errors after filtering and scaling are calculated for each grid cell and given in the web address (NASA, 2021a). In this study, monthly GRACE land water storage data produced by The Center for Space Research at Texas University, gridded and scaled by NASA Jet Propulsion Laboratory (JPL) were utilized. 98-month water storage changes from February 2010 to November 2020 were used. All data can be found with the help of (NASA, 2020b). Monthly 1° grid GRACE TWS data sets from the time-varying gravity model RL05 are contributed by the Center for Space Research (CSR) at the University of Texas, the German Research Centre for Geosciences (GFZ), and the Jet Propulsion Laboratory (JPL). Sakumura et al. (2014) found that the ensemble solution of CSR, GFZ, and JPL, using a simple arithmetic mean, can reduce the noise in the equivalent water height (EWH) by 5–10 mm (root mean square). Therefore, this ensemble solution (referred to as the TWS grid) is employed in this paper. With the exception of the spherical harmonics, the CSR Mascon solutions (CSR-M) can capture all signals observed by GRACE within the measurement noise level and can be used without further processing (Yin et al., 2020). CSR-M are provided with a spatial resolution of 0.5°. Detailed information can be found in (Save et al., 2016). In this study, the drought analysis region was determined as Turkey. The territory of Turkey is located between 36° and 42° North latitude and 26°–45° East longitude. Its shape roughly resembles a rectangle and its width is 1660 km. The actual area it covers, including lakes and islands, is 814,578 km^2, and its projection area is 783.562 km^2. When the GRACE satellite observations were examined, it was revealed that the observations in Turkey were made by point and areal. Some stations have been identified as having the same equivalent water thickness. Points with the same equivalent water thickness are designated as areas and all are numbered. The location of the study area obtained with the help of (Google Earth, 2020) is demonstrated in Fig. 1. The geographical coordinates of the points determined for the study can be also obtained from (MGM, 2020).

PERSIANN Data

At the later phases of the study, the precipitation data of the 81 points used for SPI analysis were obtained from the Precipitation Estimation from Remotely Sensed Information using the Artificial Neural Networks (PERSIANN) system developed by the Center for Hydrometeorology and Remote Sensing (CHRS) at the University of California.

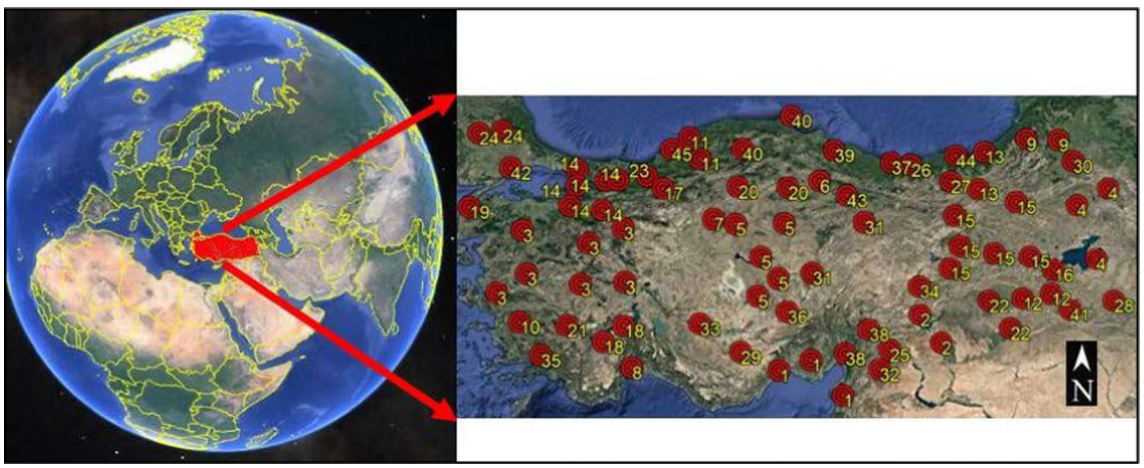


Fig. 1 Location of study area and designated regions according to GRACE data

Since Turkey consists of 81 provinces, the central coordinates of these provinces were taken as reference points. Geographical features of these points are depicted in Table 1. Detailed information about this data in PERSIANN is available in sources (Hsu et al., 1997, 1999,

Table 1 Geographical features of reference points for PERSIANN data

No	Reference point (centre of province)	Elevation (m)	Latitude (N)	Longitude (E)	No	Reference point (centre of province)	Elevation (m)	Latitude (N)	Longitude (E)
1	Adana	20	36.9838	38.2775	41	İzmir	29	38.3949	27.0819
2	Adıyaman	672	37.7553	38.2775	42	K.maraş	572	37.576	36.915
3	Afyon	1034	38.738	30.5604	43	Karabük	259	41.1963	32.6216
4	Ağrı	1646	39.7253	43.0522	44	Karaman	1018	37.1932	33.2202
5	Aksaray	970	38.3705	33.9987	45	Kars	1777	40.6042	43.1073
6	Amasya	409	40.6668	35.8353	46	Kastamonu	800	41.371	33.7756
7	Ankara	959	40.124	32.9992	47	Kayseri	1094	38.687	35.5
8	Antalya	64	36.9063	30.799	48	Kırıkkale	751	39.8433	33.5181
9	Ardahan	1827	41.1061	42.7055	49	Kırklareli	232	41.7382	27.2178
10	Artvin	613	41.1752	41.8187	50	Kırşehir	1007	39.1639	34.1561
11	Aydın	56	37.8402	27.8379	51	Kilis	640	36.7085	37.1123
12	Balıkesir	102	39.6326	27.92	52	Kocaeli	74	40.7663	29.9173
13	Bartın	33	41.6248	32.3569	53	Konya	1029	37.8687	32.4713
14	Batman	610	37.8636	41.1562	54	Kütahya	969	39.4171	29.9891
15	Bayburt	1584	40.2547	40.2207	55	Malatya	950	38.3367	38.2173
16	Bilecik	539	40.1414	29.9772	56	Manisa	71	38.6153	27.4049
17	Bingöl	1139	38.8847	40.5007	57	Mardin	1040	37.3103	40.7284
18	Bitlis	1785	38.475	42.1625	58	Mersin	7	36.7808	34.6031
19	Bolu	743	40.7329	31.6022	59	Muğla	646	37.2095	28.3668
20	Burdur	957	37.722	30.294	60	Muş	1322	38.7509	41.5023
21	Bursa	238	40.2552	29.5624	61	Nevşehir	1260	38.6163	34.7025
22	Çanakkale	6	40.141	26.3993	62	Niğde	1211	37.9587	34.6795
23	Çankırı	755	40.6082	33.6102	63	Ordu	5	40.9838	37.8858
24	Çorum	776	40.5461	34.9362	64	Osmaniye	94	37.1021	36.2539
25	Denizli	425	37.762	29.0921	65	Rize	3	41.04	40.5013
26	Diyarbakır	674	37.8973	40.2027	66	Sakarya	30	40.7676	30.3934
27	Düzce	146	40.8437	31.1488	67	Samsun	4	41.3435	36.2553
28	Edirne	51	41.6767	26.5508	68	Siirt	895	37.9319	41.9354
29	Elazığ	989	38.6443	39.2561	69	Sinop	32	42.0299	35.1545
30	Erzincan	1216	39.7523	39.4868	70	Sivas	1294	39.7437	37.002
31	Erzurum	1860	39.9058	41.2544	71	Şanlıurfa	550	37.1608	38.7863
32	Eskişehir	801	39.7656	30.5502	72	Şırnak	1350	37.5209	42.4523
33	Gaziantep	854	37.0585	37.351	73	Tekirdağ	4	40.9585	27.4965
34	Giresun	38	40.9227	38.3878	74	Tokat	611	40.3312	36.5577
35	Gümüşhane	1216	40.4598	39.4653	75	Trabzon	25	40.9985	39.7649
36	Hakkari	1727	37.5745	43.7388	76	Tunceli	981	39.1058	39.5408
37	Hatay	104	36.2048	36.1513	77	Uşak	919	38.6712	29.404
38	Iğdır	856	39.9227	44.0523	78	Van	1675	38.4693	43.346
39	Isparta	997	37.7848	30.5679	79	Yalova	4	40.6589	29.2796
40	İstanbul	99	40.8977	29.3033	80	Yozgat	1301	39.8243	34.8159
					81	Zonguldak	135	41.4492	31.7779

2000, 2002; Nguyen et al., 2019; Sorooshian et al., 2000, 2002, 2014). Data can be found at (CHRSDATA, 2021).

Atmospheric/Oceanic Climate Indexes Data

The second part of the study focused primarily on climatic oscillations affecting Turkey. It has been tried to find out whether there is a relationship between atmospheric/oceanic climate indexes and drought.

The Arctic Oscillation (AO) is an atmospheric model of circulation over the mid-high latitudes of the Northern Hemisphere. The most prominent reflection of this oscillation is the position of the storm-directed mid-latitude jet stream from north to south. AO has an impact on the climate in dense population centers in North America, Europe and Asia, especially in winter. Monthly AO data can be obtained from source (National Oceanic and Atmospheric Administration (NOAA), 2020a).

The North Atlantic Oscillation (NAO) is the sea level surface differential pressure model between Subtropical (Azores) High and Subpolar Low. Positive NAO reflects sub-normal altitudes and pressure across the high latitudes of the North Atlantic, and above-normal altitudes and pressure over the Central North Atlantic, the Eastern United States, and Western Europe. Negative NAO reflects the exact opposite pattern. Monthly NAO values can be reached from (NOAA, 2020b).

The Multivariate ENSO (El-Nino/Southern Oscillation) Index (MEI) is determined by the weighted anomaly average of 6 meteorological variables in the Tropical Pacific. These variables are sea surface temperature, sea level pressure, surface air temperature, components of surface wind and cloudiness fraction of the sky. Bi-monthly MEI values can be found at (NOAA, 2020c).

The Oceanic Nino Index is a standard index to describe the phase of the El Nino Southern Oscillation (ENSO). It is a measure of the level of abnormally hot or cold compared to the "normal" of the Pacific Ocean. This index is used to describe the stage of ENSO that has significant tele-connections all over the world. 3-month moving average values can be accessed from (NOAA, 2020d).

The Southern Oscillation Index (SOI) is a time series used to characterize large-scale sea level pressure patterns in the Tropical Pacific. Monthly data can be obtained from (NOAA, 2020e).

Method

GRACE-Based Water Storage Deficit Index (WSDI) and SPI

Obtained from monthly GRACE TWSA deviations, WSDI is employed to characterize drought formations and the severity of drought (Yirdaw et al., 2008). WSDI is obtained with the help of Eqs. (1) and (2).

$$WSD_{i,j} = TWSA_{i,j} - \overline{TWSA_{j'}} \tag{1}$$

$$WSDI_{i,j} = \frac{WSD_{i,j} - \mu}{\sigma} \tag{2}$$

$WSD_{i,j}$ and $TWSA_{i,j}$ are the total water storage deficit and GRACE-inferred TWSA time series for the jth month in the year i, respectively. $\overline{TWSA_{j'}}$ is the long term TWSA average for the same month.

μ and σ are the mean and standard deviation of the WSD time series, respectively. Negative WSD represents a deficit in total water storage, positive WSD represents a surplus in total water storage. Negative WSDs lasting for three or more consecutive months can be designated as drought events (Thomas et al., 2014). Thus, WSDI can be calculated by standardizing the WSD values. The WSDI time series represent each month's deviation from the average conditions of that month. The effect of the water storage deficit and its duration can be used to determine the severity of the drought. Total drought severity can be described with the help of Eq. 3.

$$Se(t) = M(t)xD(t) \tag{3}$$

Here, $Se(t)$ is the severity of the drought, $M(t)$ is the average water deficit in the drought event (the average of negative WSD values during the drought), and $D(t)$ is the duration that indicates how long the drought lasts (the time between the month when the drought starts and ends) (Yu et al., 2019).

As to equivalent water thickness, two-stage data processing is used to suppress the noise in the high degree and order spherical harmonics of the GRACE gravity solutions, following the approaches of (Swenson & Wahr, 2006). The monthly spherical harmonics are processed using a decorrelation filter and Gaussian smoothing. The decorrelation filter is performed in such a way that, for a given spherical harmonic order, a third-order polynomial function is derived by a least squares fit to the even or odd coefficient pairs of the GRACE solutions and is removed from the monthly solutions. The Gaussian smoothing is applied with a radius of 500 km (Yi & Wen, 2016).

SPI (McKee et al., 1993) is a meteorological drought index widely used on a global scale. The SPI is based on long-term precipitation records fitted to a probability distribution. In order to calculate the SPI, the precipitation record is first fitted to the gamma distribution and then subsequently converted to the normal distribution using the equal-probability function. In this study, monthly PERSIANN precipitation data were used to calculate SPI. Only precipitation is considered in SPI. This means that other

Table 2 WSDI/SPI drought category

WSDI/SPI	Drought category
Above 2	Extreme wet
From 1.50 to 1.99	Severe wet
From 1 to 1.49	Moderate wet
From − 0.99 to 0.99	Near-normal
From − 1 to − 1.49	Moderate drought
From − 1.50 to − 1.99	Severe drought
Below − 2	Extreme drought

meteorological factors are neglected and this situation creates a disadvantage. More detailed information on SPI can be found in (McKee et al., 1993) and (Topçu & Seçkin, 2016). In this study, SPI values of 1, 3, 6 and 12-month were calculated in order to investigate the short-term and long-term effects of precipitation. Drought category according to WSDI index values is depicted in Table 2. It can be expected that SPI/WSDI values will be within one standard deviation approximately 68 per cent of the time, within two standard deviations 95 percent of the time and within three standard deviations 99 per cent of the time. It is considered a strength for water management planning that the frequencies of the "extreme" and "severe" classifications are consistent and low for each location and time scale. An "extreme" drought on this scale (WSDI/SPI ≤ -2.0) occurs about two to three times in 100 years.

Mann–Kendall Trend Analysis

In this study, a trend analysis was conducted to determine the increase or decrease of WSD values calculated by TWSA and TWSA, derived from the GRACE satellite during the analysis period. TWSA and WSD values were examined by Mann–Kendall trend analysis. The Mann–Kendall test is performed to test H1, which is the monotonic trend of increasing or decreasing randomly clustered xi values in the time series against the null hypothesis H0. Data is organized sequentially over time. Each observation value is compared with the following observation value. Detailed information about Mann–Kendall trend analysis can be found in (Salmi et al., 2002). The correlations of commonly used climatic indices and WSDI values were examined considering that they may have an effect on drought events. Pearson's type correlation was applied in the study. Pearson correlation is a statistical method used to determine whether there is a linear relationship between two numerical measurements, if any, the direction and strength of this relationship. If the correlation coefficient is negative, there is an inverse relationship between the two variables, meaning "one of the variables increases while the other decreases".

The drought mapping was executed to reveal EWT and WSDI changes visually. It has been mapped using the Inverse Distance Weighted Interpolation Method with the help of ArcGis package program (ESRI, 2012).

The flowchart showing the process steps in the study is given in Fig. 2.

Results and Discussion

Results of Mann–Kendall Trend Analysis

The changes in TWSA and WSD values for each study area were assessed by Mann–Kendall trend analysis in the period of February 2010 to November 2020. Results are illustrated in Table 3. According to Table 3, it can be observed that there is an increase or decrease in TWSA and WSD values for each study area. As can be understood from negative Test Z (TZ), a decreasing trend stands out in almost all regions. Across Turkey, it is demonstrated that TWSA and WSD decreased at $\alpha = 0.01$ level of significance (S) and $\alpha = 0.001$ level of significance, respectively. This is the reflection of drought occurring in hydrological parameters. For WSD, an increase in the significance level of $\alpha = 0.05$ stands out in regions 12, 27 and 41. In fact, one of the consequences of climate change is that while drought increases in one region, abnormal rainfalls are observed in the other region. In the TWSA values, no significant trend was ascertained in the regions 2, 12, 15, 22, 25, 28, 32, 34, 35, 40 and 41. In terms of WSD values, no significant trend was identified in the regions 2, 22, 25, 32 and 35.

Analysis of EWT Values

Satellite-derived EWT values represent WSD. Negative values indicate water deficit and positive values report excess water. In Fig. 3, the average EWT values declined from + 1.5 to − 5.6 from February 2010 to November 2020. Especially in 2018, the average EWT value peaked at − 11.1 cm. The second peak value was − 8.2 cm in 2014. The third lowest year is 2020 with a value of − 5.6. 2020 is followed by 2019 with a value of − 3.4 cm and 2017 with a value of − 1.1 cm.

Figure 4 presents a visualized version of how Equivalent Water Thickness (EWT) has changed throughout Turkey over the years. In 2011 and 2012, there was a surplus of water on the Western Mediterranean coasts. In 2013, the water deficit in the central part of Central Anatolia became evident. Especially in 2014 and 2018, there was a decrease in the equivalent water thicknesses across Turkey. In 2015, a water deficit occurred in the south of Eastern Anatolia. In 2016, the Eastern Mediterranean experienced a water shortage. The areas most affected by this decrease were Eastern Anatolia and Southeast Anatolia regions of Turkey. The least

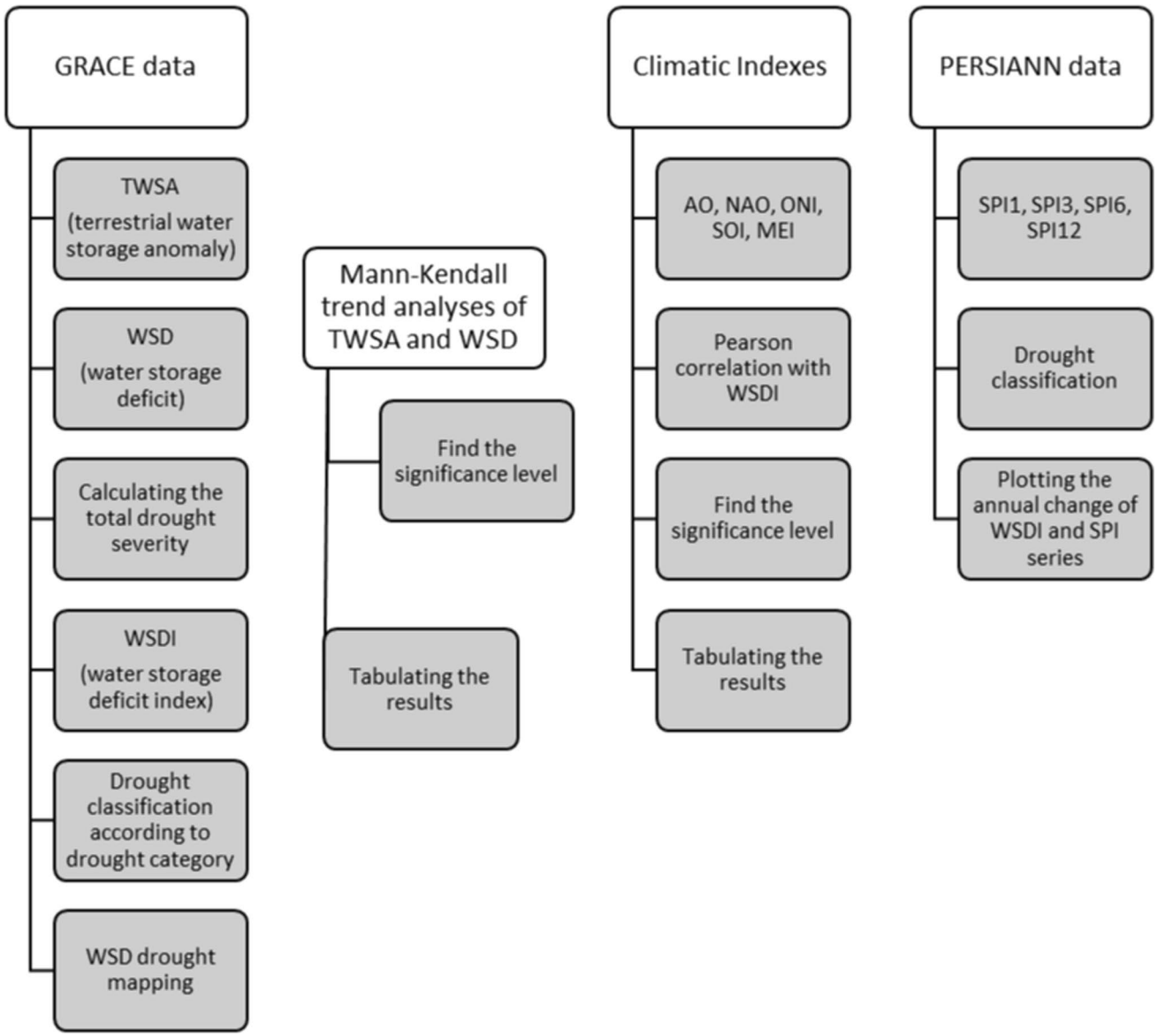


Fig. 2 Flowchart of the study

equivalent water thickness was in 2018. When the data of 2020 are examined, it is apparent that the north of the Inner Aegean and Northeast Anatolia regions are the regions most affected by drought.

Results of WSDI

Figure 5 highlighted that it has been transitioned to the dry period across Turkey since 2014. The trend line on the chart also supports this. While the minimum WSDI value was − 2.0913 in 2014, the maximum WSDI value was observed in 2013 with 1.280245.

Table 4 summarized TS and AD values occurring across Turkey. Table 4 demonstrated that the longest drought was experienced in 2014 and 2020. TS is simply a mathematical expression to determine the severity of the drought. Again, Table 4 highlighted that peak deficit values were seen especially in February, April, July and November.

Figure 6 presents the areal variation of the WSD values throughout Turkey. According to the maps, the western Mediterranean part of Turkey in 2011, the Mediterranean region and South of the Central Aegean in 2012 is moderately wet. In 2013, everywhere except the Middle Black Sea region is on the limit of drought. When 2014 is examined, moderate drought is observed in the Black Sea region, Eastern Mediterranean, Southeastern Anatolia and the west of Eastern Anatolia, while other regions are on the drought border line. In 2018, moderate drought prevailed in Eastern

Table 3 Trend analysis results for TWSA and WSD

Region-TWSA						Region-WSD					
	S	TZ		S	TZ		S	TZ		S	TZ
1	***	−3.63	24	**	−3.22	1	***	−3.56	24	***	−4.86
2	X	−1.06	25	X	−1.21	2	X	−1.07	25	X	−1.28
3	***	−4.54	26	**	−2.9	3	***	−7.28	26	***	−6.55
4	***	−4.06	27	**	−2.65	4	***	−7.25	27	***	−5.94
5	***	−3.57	28	X	0.76	5	***	−5.87	28	*	1.98
6	*	−1.94	29	***	−4.81	6	**	−3.11	29	***	−5.39
7	**	−2.91	30	***	−5.55	7	***	−5.5	30	***	−8.75
8	***	−6.16	31	*	−2.03	8	***	−6.38	31	***	−3.63
9	***	−6.63	32	X	−0.38	9	***	−8.74	32	X	0.34
10	*	−2.54	33	***	−5.68	10	***	−3.35	33	***	−6.42
11	*	−2.01	34	X	−1.57	11	**	−3.16	34	**	−3.25
12	X	1.1	35	X	−0.33	12	*	2.5	35	X	−0.39
13	**	−3.06	36	***	−3.81	13	***	−6.37	36	***	−4.39
14	***	−4.16	37	***	−3.29	14	***	−7.5	37	***	−7.08
15	X	−1.33	38	**	−3.03	15	*	−2.26	38	***	−3.65
16	*	−2.3	39	***	−3.33	16	***	−4.95	39	***	−6.47
17	***	−3.3	40	X	−1.6	17	***	−6.62	40	*	−2.19
18	***	−6.12	41	X	0.92	18	***	−8.02	41	*	2.28
19	***	−3.75	42	***	−4.24	19	***	−5.98	42	***	−6.86
20	*	−2.46	43	**	−2.54	20	***	−4.1	43	***	−5.68
21	***	−4.33	44	*	−2.54	21	***	−5.76	44	***	−6.02
22	X	−0.98	45	**	−2.93	22	X	−1.05	45	***	−6.18
23	***	−3.3	TURKEY	**	−3.21	23	***	−6.62	TURKEY	***	−7.02

***if trend at α = 0.001 level of significance

**if trend at α = 0.01 level of significance

*if trend at α = 0.05 level of significance

X: no trend

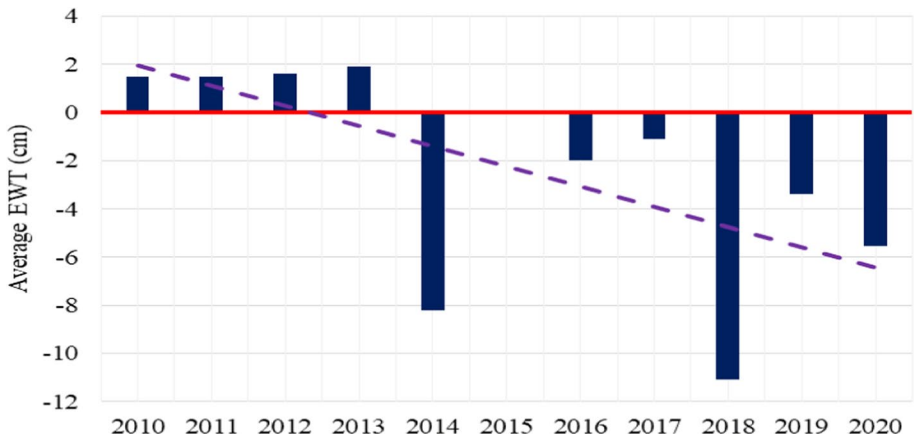


Fig. 3 EWT average values throughout Turkey

Anatolia, excluding its northern part. When the data of 2020 are examined, moderate drought was observed in Northeast Anatolia, Marmara and Aegean regions.

In Table 5, it can be inferred that in the regions, WSDI and ONI values have negative correlations at high significance level.

Figure 7 includes a graphical comparison of WSDI and correlated climatic indexes with a 0.05 significance level throughout Turkey. WSDI values and AO, NAO and ONI values have negative correlations at 0.05 significance level. This illustrates that while the climatic index values increase (decrease), the WSDI values decrease (increase).

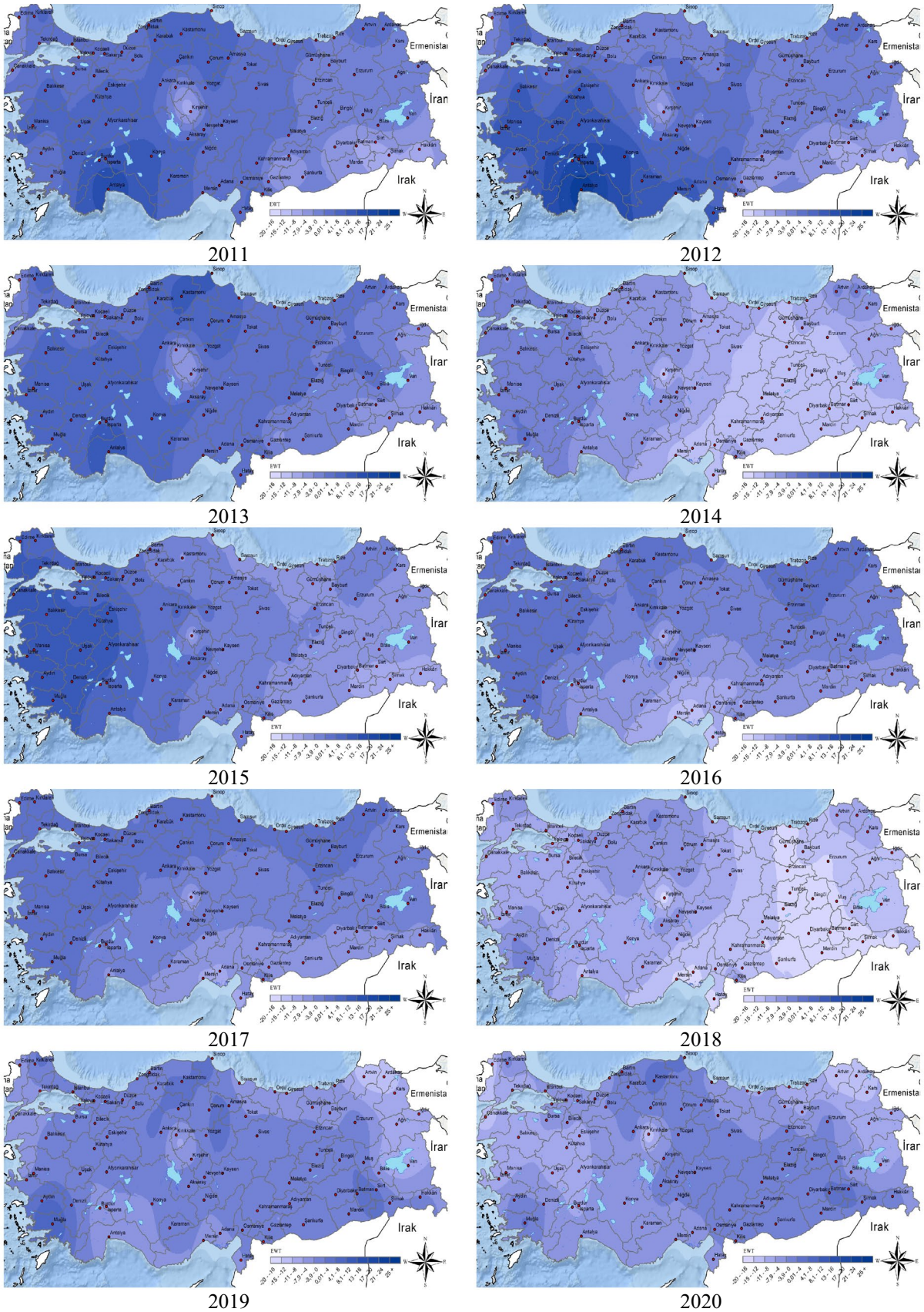


Fig. 4 Change in EWT values throughout Turkey

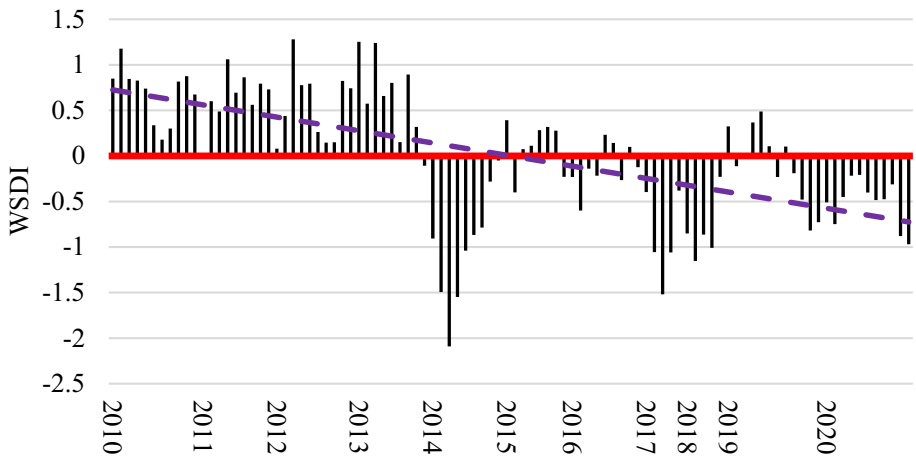


Fig. 5 Annual change in the WSD value for Turkey

Table 4 Drought severity table for Turkey

TURKEY				
Time Period	**Duration (month)**	**Total Severity (TS)(cm)**	**Average Deficit (AD)(cm)**	**Peak Deficit (cm) (period/value)**
2014/01-2014/11	11	-59.45027	-5.40457	2014/04/-11.3963
2016/01-2016/05	5	-8.61729	-1.72346	2016/02/-3.38737
2017/01-2017/06	6	-29.5759	-4.92931	2017/04/-8.46775
2018/06-2018/12	7	-32.5507	-4.6501	2018/07/-6.45073
2019/09-2019/12	4	-13.2962	-3.32406	2019/11/-4.74993
2020/01-2020/11	11	-38.2816	-3.19013	2020/11/-5.64584

When the AO received a strong negative value, low pressure occurs in continental Europe and the Mediterranean basin, so Turkey will remain under the influence of low pressure in front and southern winds. Warm and rainy days are seen in Turkey. In case of strong positive value, high pressure dominance occurs in the Mediterranean basin, so that Turkey experiences a shortage of precipitation. During the close to neutral AO index values, Turkey might encounter many situations such as cold and rainy weather, non-cryogenic rainy weather, dry (precipitation-free) weather etc. The effects of the NAO index are similar to the effects of AO on Turkey (Türkeş & Erlat, 2005). When the AO and WSDI chart is analyzed, it can be determined that the WSDI values are positive in the parts where AO is very low. Again, the same scheme applies to NAO and ONI.

In the final stage of the study, the comparison of SPI and WSDI, which is one of the meteorological drought indexes, was made. In this study, the aim of comparing WSDI and SPI values is to compare drought index values obtained from satellite data and surface measurements. However, since WSDI is calculated with TWSA, which includes many hydrological variables, it is more likely to give accurate answers in drought analysis. SPI values of 1, 3 and 6 months can be used to define meteorological drought in the short term, and SPI values of 12 and more months can be used to describe hydrological drought. While the lack of precipitation can be felt immediately in the soil, hydrological drought takes longer to take effect. Therefore, SPI values are calculated for different periods. According to Fig. 8, WSDI and SPI values tend to increase between 2013 and 2014, and decrease between 2014 and 2015. WSDI and SPI values follow opposite directions between 2012 and 2013. This difference may be due to the terrestrial water storage used in the WSDI calculation. This is because terrestrial water storage takes into account both surface water and groundwater. SPI, on the other hand, is calculated only with atmospheric precipitation. Surface waters include dams and artificial ponds. Therefore, even if precipitation decreases, surface water can be increased by supplementation from various nearby hydrological sources. The high number of dams and the use of drinking water from these dams also increases the groundwater level. Because the amount of water drawn from water wells is decreasing. The difference between WSDI and SPI between 2012 and 2013 may have occurred due to the aforementioned situation. After 2018, it can be identified that both WSDI and SPI values tend to increase, but towards the end of 2020 they decreased in the direction of drought.

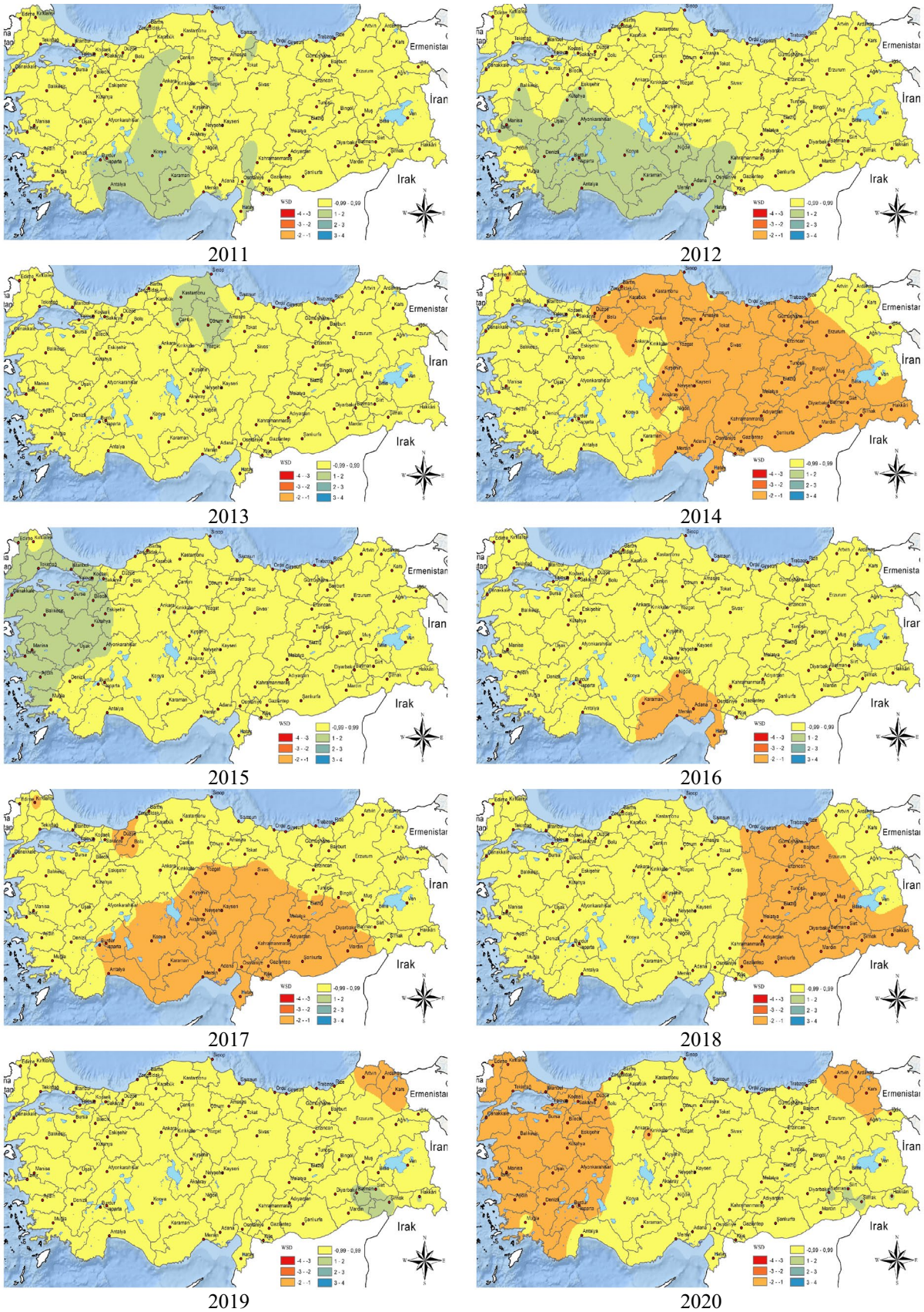


Fig. 6 WSD drought maps throughout Turkey

Table 5 Correlation table of WSDI and climatic indexes

Region	AO	MEI	NAO	ONI	SOI	Region	AO	MEI	NAO	ONI	SOI
1		**		**		24	*				
2			*	*		25		*	*	**	
3	*					26	**		**	**	
4	*			*		27	*		**	*	
5	No correlation					28	No correlation				
6		*		**	++	29		**		**	
7		*		**	++	30	*			*	
8		**		**	+	31	*			*	
9	No correlation					32		*		*	
10	**	++		+	**	33		**		**	*
11		**		**	++	34	*		*		
12	No correlation					35	**	++		++	**
13	*		**	*		36		*		**	
14	*					37	*		**	**	+
15	*		*			38		**		**	
16	*					39		**	*	**	++
17	No correlation					40		**		**	++
18				*		41	No correlation				
19	**					42	*				
20		*		**	++	43		*	*	**	++
21	*					44	**		**	*	
22	*		*			45					*
23	No correlation					TURKEY	*		*	*	

**Negative correlation is significant at the 0.01 level (2-tailed)

*Negative correlation is significant at the 0.05 level (2-tailed)

++Positive correlation is significant at the 0.01 level (2-tailed)

+Positive correlation is significant at the 0.05 level (2-tailed)

With the thought that there might be a correlation in terms of drought among SPI-1, SPI-3, SPI-6, SPI-12 values calculated together with monthly total precipitation values obtained from PERSIANN data and 5 different climatic oscillation indexes, Pearson correlation was applied. According to the results, it was revealed that only SPI-12 values and MEI and ONI values were correlated at a 0.05 significance level. Therefore, only the changes of SPI-12 periods with MEI and ONI are depicted in Fig. 9.

The GRACE terrestrial water storage anomaly (TWSA) is used in various hydrological studies from large river basins to global scale, predicting water storage changes and flow, groundwater changes, ice mass losses, regional flood potential and regional water management, including drought (Thomas et al., 2014). TWS is a fundamental component of the hydrological cycle in land areas and represents the total amount of water stored under and above ground. TWS consists of surface water (SW) including lakes, snow water equivalent, ground moisture, groundwater storage, canopy water, and glaciers. The GRACE satellite measured the global TWS changes from April 2002 to June 2017. The GRACE-FO satellite continues to measure as well. Today, TWS has attracted worldwide attention due to the availability of clean water and its relationship with the sustainability of global water resources (Liu et al., 2019). Monthly changes observed in gravity are due to monthly changes in masses. Mass changes can be thought of as the change of a very thin layer of water thickness concentrated near the surface of the earth. In fact, most of the monthly gravitational changes are actually due to changes in the amount of water in hydrological reservoirs, movement of the ocean, atmospheric and black glacial masses, and changes between these masses. The vertical dimension of these changes is calculated with the equivalent water thickness in centimeters. Some changes in gravity are caused by the displacement of glacial areas or by the redistribution of mass in land and ocean as a result of earthquakes (Chambers, 2006; Chambers & Bonin, 2012); Cheng & Tapley, 2004; Linage et al., 2009; Swenson & Wahr, 2006; Swenson et al., 2008; Wahr et al., 1998. Equivalent water thickness is a measure of ecosystem water status and an important parameter for ecosystem dynamics studies, fire potential and biological responses to climate change.

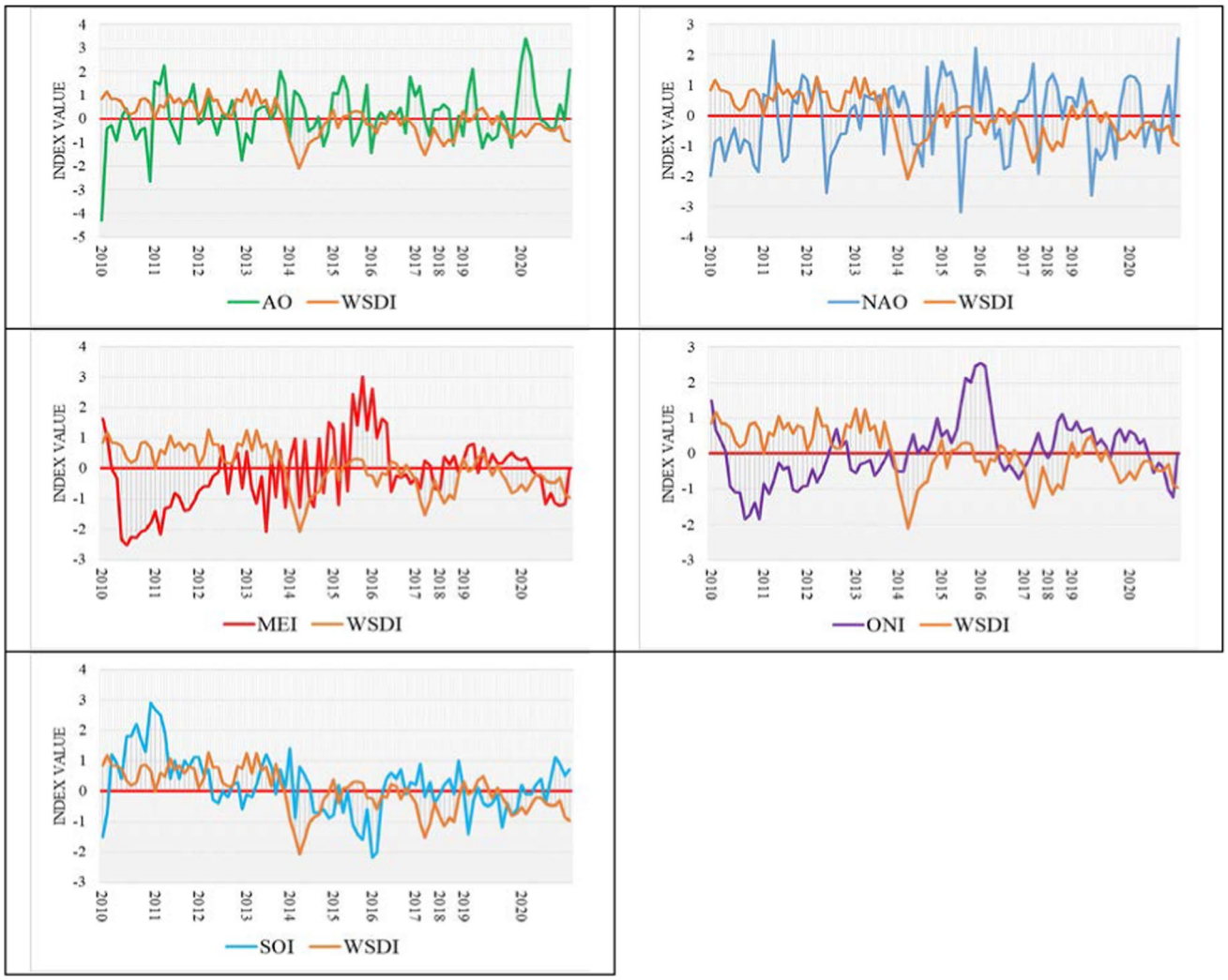


Fig. 7 WSD and correlated climatic parameters' annual change in Turkey

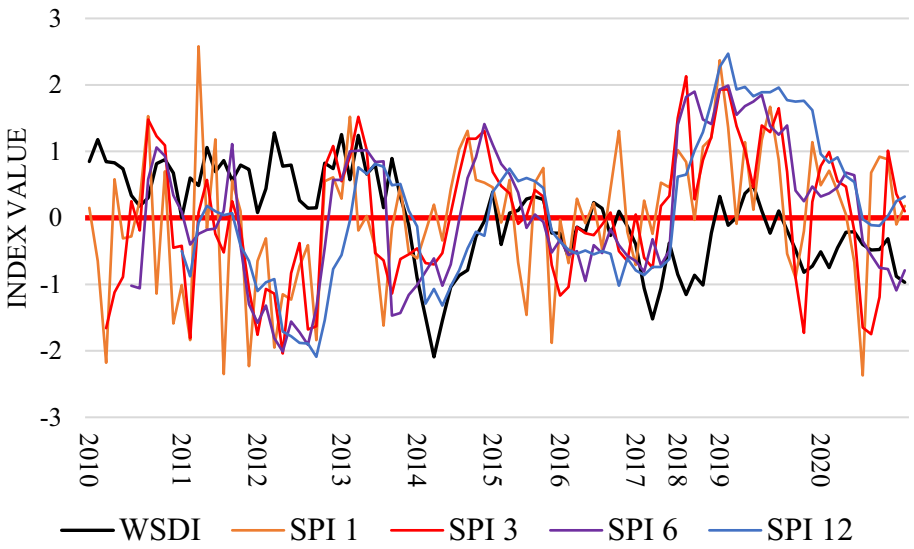


Fig. 8 Annual change of WSDI and SPI series in Turkey

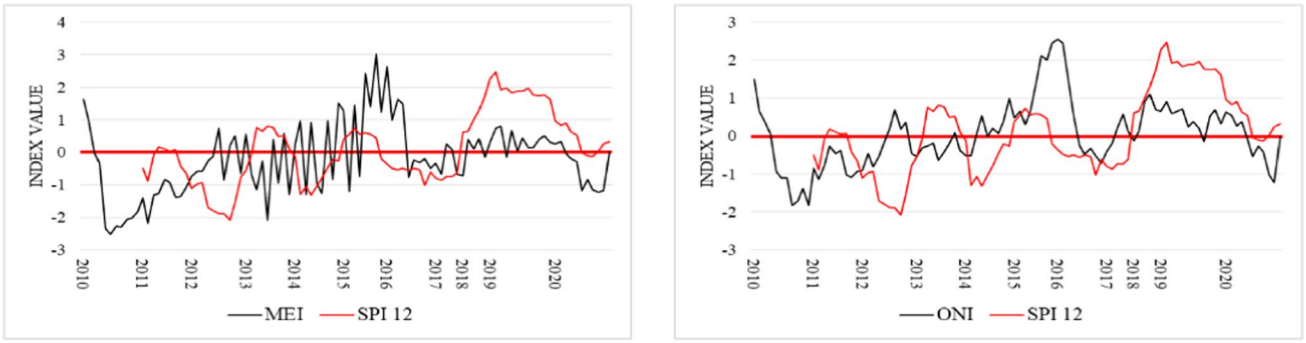


Fig. 9 The change of SPI-12 periods with MEI and ONI

Conclusion

The decade between 2011 and 2020 was the hottest decade ever measured. The year of 2020 was 0.6 °C warmer than the 1981–2010 reference period (COPERNICUS, 2020). For this reason, the drought analysis of the last 10 years has been carried out in this study. It is evident that GRACE satellites have contributed significantly to the field of hydrology by revealing large-scale information on groundwater consumption and drought. WSD and WSDI values have been used to analyze the drought events in Turkey. Additionally, WSDI values were compared with SPI values of 1, 3, 6 and 12 months, similarities and differences in drought classification were discussed. Differences in calculation methods, data and drought severity levels made a difference between SPI and WSDI. According to the results of this study, the TWS values throughout Turkey has two turning points; Wet period from 2010 to 2014, dry period from 2014 to 2020. Equivalent water thickness also decreased from positive values to negative values. According to the WSD results, 6 dry periods were detected throughout Turkey (2014–2020). The most severe drought occurred in 2014 and then in 2020. The drought continued for 11 months in 2014 and 2020. Within the scope of the study, WSDI and SPI values were also compared with atmospheric/oceanic climatic indexes affecting the Earth and Turkey. The aim is to predict drought events based on climatic indexes. However, it was revealed that the WSDI values among 5 different indexes could be mostly related to AO, NAO and ONI values throughout Turkey. In the regional analysis, it was determined that ONI values and WSDI values were correlated at a high level of significance. TWSA values obtained from GRACE satellites accurately detected the 2014, 2018 and 2020 droughts. For this reason, more reliable satellite data can be used instead of sparse hydro-meteorological stations in very large areas. This study is expected to shed light on the planned water management projects in the regional areas within the scope of the study and throughout Turkey.

Author contributions This study was conceived by Topçu and all of the analysis and drafting of the manuscript was conducted by Topçu.

Funding There is no funding for this research study.

Data availability The data used in this research will not be available.

Code availability Not applicable.

Declarations

Conflict of interest The author declare that they have no conflict of interest.

Ethical approval There are no ethical issues in this study.

Consent for publication The author agree to the publication of thisresearch and the copyright statement.

Consent to participate This research has been approved by author and signed on the signature.

References

Ahi, O. G., & Jin, S. (2019). Hydrologic mass changes and their implications in mediterranean-climate Turkey from GRACE measurements. *Remote Sensing, 11*, 120. https://doi.org/10.3390/rs11020120

Chambers, D. P. (2006). Observing seasonal steric sea level variations with GRACE and satellite altimetry. *Journal of Geophysical Research, 111*(C3), C03010. https://doi.org/10.1029/2005JC002914

Chambers, D. P., & Bonin, J. A. (2012). Evaluation of release 05 time-variable gravity coefficients over the ocean. *Ocean Science, 8*, 859–868. https://doi.org/10.5194/os-8-859-2012

Chen, J. L., Rodell, M., Wilson, C. R., & Famiglietti, J. S. (2005). Low degree spherical harmonic influences on gravity recovery and climate experiment (GRACE) water storage estimates. *Geophysical Research Letters, 32*(L14405), 2005a. https://doi.org/10.1029/2005GL022964

Cheng, M., & Tapley, B. D. (2004). Variations in the Earth's oblateness during the past 28 years. *Journal of Geophysical Research: Solid Earth, 109*, B9. https://doi.org/10.1029/2004JB003028

CHRSDATA. (2021). Retrieved February 10, 2020, from https://chrsdata.eng.uci.edu/

COPERNICUS. (2020). Retrieved December 10, 2020, from https://climate.copernicus.eu/2020-warmest-year-record-europe-globally-2020-ties-2016-warmest-year-recorded

Environmental Systems Research Institute (ESRI). (2012). ArcView GIS version 10.1. A computer software to visualize, explores, query and analyze data spatially, USA.

GOOGLE EARTH. (2020). Retrieved December 10, 2020, from https://www.google.com/intl/tr/earth/

Gürsoy, S. (2018). *An investigation of climate indices via signal analysis methods, Master's Thesis*, Hacettepe University, Ankara.

Hosseini-Moghari, S. Y., Araghinejad, S., Ebrahimi, K., Tang, Q., & Aghakouchak, A. (2020). Using GRACE satellite observations for separating meteorological variability from anthropogenic impacts on water availability. *Scientific Reports, 10*, 15098. https://doi.org/10.1038/s41598-020-71837-7

Hsu, K., Gao, X., Sorooshian, S., & Gupta, H. V. (1997). Precipitation estimation from remotely sensed information using artificial neural networks. *Journal of Applied Meteorology, 36*(9), 1176–1190. https://doi.org/10.1175/1520-0450(1997)036<1176:PEFRSI>2.0.CO;2

Hsu, K., Gupta, H. V., Gao, X., & Sorooshian, S. (1999). Estimation of physical variables from multiple channel remotely sensed imagery using a neural network: Application to rainfall estimation. *Water Resources Research, 35*(5), 1605–1618. https://doi.org/10.1029/1999WR900032

Hsu, K., Gupta, H. V., Gao, X., & Sorooshian, S. (2000). Rainfall estimation from satellite imagery. In R. S. Govindaraju & A. R. Rao (Eds.), *artificial neural networks in hydrology* (pp. 209–234). Kluwer Academic Publishers.

Hsu, K., Gupta, H. V., Gao, X., Sorooshian, S., & Imam, B. (2002). SOLO-An artificial neural network suitable for hydrologic modelling and analysis. *Water Resources Research, 38*(12), 1302.

Khorrami, B., Ali, S., Abadi, L. H., & Jehanzaib, M. (2023). Spatio-temporal variations in characteristics of terrestrial water storage and associated drought over different geographic regions of Türkiye. *Earth Science Informatics, 16*, 717–731. https://doi.org/10.1007/s12145-022-00907-3

Landerer, F. W., & Swenson, S. C. (2012). Accuracy of scaled GRACE terrestrial water storage estimates. *Water Resources Research, 48*, W04531. https://doi.org/10.1029/2011WR011453

Lenk, O. (2013). Satellite based estimates of terrestrial water storage variations in Turkey. *Journal of Geodynamics, 67*, 106–110.https://doi.org/10.1016/j.jog.2012.04.010

Linage, C., Rivera, L., Hinderer, J., Boy, J. P., Rogister, Y., Lambotte, S., & Biancale, R. (2009). Separation of coseismic and postseismic gravity changes for the 2004 Sumatra-Andaman earthquake from 4.6 yr of GRACE observations and modelling of the coseismic change by normal-modes summation. *Geophysical Journal International, 176*, 695–714. https://doi.org/10.1111/j.1365-246X.2008.04025.x

Liu, X., Feng, X., Ciais, P., & Fu, B. (2019). Widespread decline in terrestrial water storage and its link to tele-connections across Asia and Eastern Europe. *Hydrology and Earth System Sciences,* https://doi.org/10.5194/hess-2019-281

McKee, T. B., Doesken, N. J., & Kleist, J. (1993). The relationship of drought frequency and duration to time scales. In *Proceedings of the 8th Conference on Applied Climatology*, American Meteorological Society Boston, Boston, MA, USA.

MGM. (2020). Retrieved December 10, 2020, from http://www1.mgm.gov.tr/kurumsal/istasyonlarimiz.aspx

NASA. (2020b). Retrieved January 6, 2020, from http://grace.jpl.nasa.gov/data/get-data/monthly-mass-gridsland

NASA. (2021a). Retrieved January 16, 2020, from https://grace.jpl.nasa.gov/data/data-analysis-tool/

Nguyen, P., Shearer, E. J., Tran, H., Ombadi, M., Hayatbini, N., Palacios, T., Huynh, P., Updegraff, G., Hsu, K., Kuligowski, B., Logan, W. S., & Sorooshian, S. (2019). The CHRS data portal, an easily accessible public repository for PERSIANN global satellite precipitation data. *Nature Scientific Data, 6*, 180296. https://doi.org/10.1038/sdata.2018.296

NOAA. (2020a). Retrieved December 10, 2020, from https://www.cpc.ncep.noaa.gov/products/precip/CWlink/daily_ao_index/ao.shtml

NOAA. (2020b). Retrieved December 10, 2020, from https://www.cpc.ncep.noaa.gov/products/precip/CWlink/pna/nao.shtml

NOAA. (2020c). Retrieved December 10, 2020, from https://psl.noaa.gov/enso/mei/

NOAA. (2020d). Retrieved December 10, 2020, from https://origin.cpc.ncep.noaa.gov/products/analysis_monitoring/ensostuff/ONI_v5.php /

NOAA. (2020e). Retrieved December 10, 2020, from https://www.ncdc.noaa.gov/teleconnections/enso/indicators/soi/

Sakumura, C., Bettadpur, S., & Bruinsma, S. (2014). Ensemble prediction and intercomparison analysis of GRACE time-variable gravity field models. *Geophysical Research Letters, 41*, 1389–1397. https://doi.org/10.1002/2013gl058632

Salmi, T., Maata, A., Antilla, P., Ruoho-Airola, T., & Amnell, T. (2002). *Detecting trend of annual values of atmospheric pollutants by the Mann-Kendall test and Sen's slope estimates—the Excel template application Makesens* (p. 35). Finnish Meteorological Institute.

Save, H., Bettadpur, S., & Tapley, B. D. (2016). High-resolution CSR GRACE RL05 mascons. *Journal of Geophysical Research: Solid Earth, 121*, 7547–7569. https://doi.org/10.1002/2016jb013007

Sinha, D., Syed, H. T., Famiglietti, S. J., Reager, T. J., & Thomas, C. R. (2017). Characterizing drought in India using GRACE observations of terrestrial water storage deficit. *Journal of Hydrometeorology, 38*, 381–396. https://doi.org/10.1175/JHM-D-16-0047.1

Sorooshian, S., Gao, X., Hsu, K., Maddox, R. A., Hong, Y., Imam, B., & Gupta, H. V. (2002). (2002). Diurnal variability of tropical rainfall retrieved from combined GOES and TRMM satellite information. *Journal of Climate, 15*, 983–1001. https://doi.org/10.1175/1520-0442(2002)015<0983:DVOTRR>2.0.CO;2

Sorooshian, S., Hsu, K., Gao, X., Gupta, H. V., Imam, B., & Braithwaite, D. (2000). Evaluation of PERSIANN system satellite-based estimates of tropical rainfall. *Bulletin of the American Meteorology Society, 81*(9), 2035–2046. https://doi.org/10.1175/1520-0477(2000)081<2035:EOPSSE>2.3.CO;2

Sorooshian, S., Nguyen, P., Sellars, S., Braithwaite, D., Aghakouchak, A., & Hsu, K. (2014). Satellite-based remote sensing estimation of precipitation for early warning systems. *Disaster Risks and Societal Implications* (pp. 99–111). Cambridge University Press.

Sun, Z., Zhu, X., Pan, Y., Zhang, J., & Liu, X. (2018). Drought evaluation using the GRACE terrestrial water storage deficit over the Yangtze River Basin, China. *Science of the Total Environment, 634*, 727–738. https://doi.org/10.1016/j.scitotenv.2018.03.292

Swenson, S. C., Chambers, D. P., & Wahr, J. (2008). Estimating geocenter variations from a combination of GRACE and ocean model output. *Journal of Geophysical Research: Solid Earth, 1*, 2. https://doi.org/10.1029/2007JB005338

Swenson, S., & Wahr, J. (2003). Monitoring changes in continental water storage with GRACE. *Space Science Reviews, 108*, 345–354. https://doi.org/10.1023/A:1026135627671

Swenson, S. C., & Wahr, J. (2006). Post-processing removal of correlated errors in GRACE data. *Geophysical Research Letters, 33*, L08402. https://doi.org/10.1029/2005GL025285

Tang, J., Cheng, H., & Liu, L. (2014). Assessing the recent droughts in southwestern China using satellite gravimetry. *Water Resources Research, 50*, 3030–3038. https://doi.org/10.1002/2013WR014656

Thomas, C. A., Reager, T. J., Famiglietti, S. J., & Rodell, M. (2014). A GRACE-based water storage deficit approach for hydrological

drought characterization. *Geophysical Research Letters, 41*, 1537–1545. https://doi.org/10.1002/2014GL059323

Topçu, E., & Seçkin, N. (2016). Drought analysis of the seyhan basin by using standardized precipitation index (SPI) and L-moments. *Journal of Agricultural Sciences, 22*, 196–215. https://doi.org/10.1501/Tarimbil_0000001381

Türkeş, M., & Erlat, E. (2005). Climatological responses of winter precipitation in Turkey to variability of the North Atlantic oscillation during the period 1930–2001. *Theoretical and Applied Climatology, 81*, 45–69. https://doi.org/10.1007/s00704-004-0084-1

Wahr, J., Molenaar, M., & Bryan, F. (1998). Time-variability of the Earth's gravity field: Hydrological and oceanic effects and their possible detection using GRACE. *Journal of Geophysical Research: Solid Earth, 103*, 30205–30229. https://doi.org/10.1029/98JB02844

Wahr, J., Swenson, S., Zlotnicki, V., & Velicogna, I. (2004). Time variable gravity from GRACE: First results. *Geophysical Research Letters, 31*, L11501. https://doi.org/10.1029/2004GL019779

Yi, H., & Wen, L. (2016). Satellite gravity measurement monitoring terrestrial water storage change and drought in the continental United States. *Scientific Reports, 6*, 19909. https://doi.org/10.1038/srep19909

Yin, W., Hu, L., Zheng, W., Jiao, J. J., Han, S.-C., & Zhang, M. (2020). Assessing underground water exchange between regions using GRACE data. *Journal of Geophysical Research: Atmospheres, 125*, e2020JD032570. https://doi.org/10.1029/2020JD032570

Yirdaw, S. Z., Snelgrove, K. R., & Agboma, C. O. (2008). GRACE satellite observations of terrestrial moisture changes for drought characterization in the Canadian Prairie. *Journal of Hydrology, 356*, 84–89. https://doi.org/10.1016/j.jhydrol.2008.04.004

Yu, W., Li, Y., Cao, Y., & Schillerberg, T. (2019). Drought Assessment using GRACE Terrestrial Water Storage Deficit in Mongolia from 2002 to 2017. *Water, 11*, 1301. https://doi.org/10.3390/w11061301

Zhao, M., Gerua, A., Velicogna, I., & Kimball, S. J. (2017). A global gridded dataset of GRACE drought severity index for 2002–14: Comparison with PDSI and SPEI and a case study of the Australia Millennium Drought. *Journal of Hydrometeorology, 8*, 2117–2129. https://doi.org/10.1175/JHM-D-16-0182.1

Publisher's Note Springer Nature remains neutral with regard to jurisdictional claims in published maps and institutional affiliations.

Springer Nature or its licensor (e.g. a society or other partner) holds exclusive rights to this article under a publishing agreement with the author(s) or other rightsholder(s); author self-archiving of the accepted manuscript version of this article is solely governed by the terms of such publishing agreement and applicable law.